frontiers | Frontiers in Materials

TYPE Original Research
PUBLISHED 15 May 2024
DOI 10.3389/fmats.2024.1413907

OPEN ACCESS

EDITED BY
Faiz Uddin Ahmed Shaikh,
Curtin University, Australia

REVIEWED BY
Shengwen Tang,
Wuhan University, China
Guojian Liu,
Suzhou University of Science and Technology, China

*CORRESPONDENCE
Wenjin Di,
wjdi@xjau.edu.cn
Bowen Guan,
bguan@chd.edu.cn

RECEIVED 08 April 2024
ACCEPTED 30 April 2024
PUBLISHED 15 May 2024

CITATION
Li Z, Zhao Z, Ma F, Di W, Cao X, He Z and Guan B (2024), Feasibility study of replacing part of cement by igneous rock powder as cementitious material: based on mortar macroscopic properties and microstructure. *Front. Mater.* 11:1413907. doi: 10.3389/fmats.2024.1413907

Feasibility study of replacing part of cement by igneous rock powder as cementitious material: based on mortar macroscopic properties and microstructure

Zhi Li[1], Zhenhua Zhao[1], Fushan Ma[1], Wenjin Di[2,3]*, Xuanhao Cao[2], Zhenqing He[2] and Bowen Guan[2]*

[1]China First Highway Engineering Co., Ltd., Beijing, China, [2]School of Materials Science and Engineering, Chang'an University, Xi'an, China, [3]School of Transportation and Logistics Engineering, Xinjiang Agricultural University, Urumqi, China

To address the increasing demand for cement and promote sustainable development, the utilization of igneous rock powder as a supplementary material to partially replace cement has emerged as an effective strategy. In this study, the fluidity and mechanical properties of the igneous rock powder-cement (IRP-OPC) composite system were investigated, and the hydration product and microstructure of IRP-OPC were analyzed by using TG/DSC, N_2 adsorption-desorption curve (BET) and SEM. The experimental findings demonstrate that the performance of the andesite powder-cement composite cementing system (AP-OPC) surpasses that of tuff powder-cement slurry (TP-OPC) and granite powder-cement slurry (GP-OPC). When the dosage of andesite powder (AP) is 5%–15%, the flowability, flexural strength and compressive strength of cement mortar are improved. When the dosage is 10%, the 28-day compressive strength is 48.3 MPa. Under the condition of low content (10%), part of $Ca(OH)_2$ is fully consumed by active SiO_2 in AP and reacts to form C-S-H. Hydration products and AP particles with small particle size are filled into the structural gap, which refines the pore structure of cement slurry, and the increase in compactness provides support for the development of strength in the later stage. The use of 5%–15% AP instead of OPC can improve fluidity and meet the strength requirements of P.O 42.5 Portland cement. This substitution not only reduces engineering costs but also enhances resource utilization.

KEYWORDS

igneous rock powder, fluidity, compressive strength, hydration production, microstructure

1 Introduction

With the continuous development of economy, the construction of railway, road and other transportation infrastructure continues to expand, the demand for cement concrete has increased significantly. As a primary component of concrete, cement requires a significant quantity of mineral resources during its production and transportation phases, leading to the emission of substantial amounts of CO_2 gas and other pollutants.

TABLE 1 The chemical composition of raw materials.

Material	CaO	SiO_2	Al_2O_3	Fe_2O_3	SO_3	MgO	K_2O	Na_2O	TiO_2	P_2O_5	Other
TP	37.32	27.16	3.24	0.99	0.04	30.68	0.13	0.19	0.15	0.07	0.03
AP	1.92	71.72	16.19	2.21	0.18	1.27	4.43	1.6	0.25	0.08	0.15
GP	4.65	67.17	13.86	2.61	0.03	2.43	4.66	3.74	0.4	0.19	0.26

TABLE 2 Mixture proportion of igneous rock powder-cement paste.

Sample	Wate-binder ratio	Cement/%	Tuff powder/%	Granite powder/%	Andesite powder/%
#OPC	0.5	100	0	0	0
TP10		90	10	0	0
TP30		70	30	0	0
GP10		90	0	10	0
GP30		70	0	30	0
AP10		90	0	0	10
AP30		70	0	0	30

Consequently, the cement industry is characterized by its high energy consumption and environmental pollution (Bentz et al., 2017). The use of mineral admixtures to replace part of cement can reduce the environmental pollution of cement production and promote the utilization of resources, which is an effective way to promote sustainable development (Menéndez et al., 2003; Ahmad et al., 2018). As the main auxiliary cementing materials, fly ash and mineral powder have uneven geographical distribution, and a series of economic problems such as transportation cost should be considered in the construction of infrastructure in remote areas. Therefore, it is urgent to find a mineral admixture that can meet the performance requirements of Portland cement as an auxiliary cementing material to reduce the engineering cost.

Igneous rocks, also known as magmatic rocks, are one of the three main types of rocks that make up the Earth's lithosphere. According to statistics, igneous rocks account for 66% of the entire crust volume and are widely distributed (Antolik et al., 2023). Relevant studies (Piasta et al., 2016; Qaidi et al., 2022; Dobiszewska et al., 2023) have shown that some igneous rocks have certain pozzolanic activity after being processed to a certain fineness, and their active components SiO_2 and Al_2O_3 can hydrate with cement clinker to produce calcium hydroxide and high-alkaline hydrated calcium silicate, and high-quality low-alkaline hydrated calcium silicate and hydrated calcium aluminate. Andesite, tuff and granite are all igneous minerals with volcanic activity, so it is necessary to study the effect of cement on the properties of the igneous rock powder.

The application of stone powder in cement-based materials has been widely concerned by many scholars. Li (Ying et al., 2013) found that $5Mg(OH)_2{\cdot}MgCl_2{\cdot}8H_2O$ (P5) and dense microstructure are conducive to the water absorption and filling of granite waste fine particles in slurry. The content ratio and microstructure of P5 to $Mg(OH)_2$ (MH) are important factors affecting the compressive strength of mortar. Wang (Wang et al., 2023) conducted an in-depth analysis of the early 72 h hydration process and mechanical strength of the granite stone powder slurry. Compared with the control group, the hydration process acceleration rate of the granite stone powder slurry system was delayed. The addition of granite stone powder to manufactured sand concrete resulted in a decrease in mechanical properties at all ages, and the amount of incorporation should be controlled within 10%. Elmoaty (Elmoaty, 2013) found that the compressive strength of concrete can be improved when 5% granite powder is used instead of cement. Liu (Liu SH. et al., 2021) found that the early hydration rate and cumulative hydration heat release of cement paste were reduced by tuff powder, and the pozzolanic activity of tuff powder could be improved by thermal curing conditions, while the early hydration degree of composite system could be improved by the alkalinity of tuff powder, resulting in the early compressive strength. Liu (Liu et al., 2022) found that the 7-day bending strength of cement slurry can be improved when the content of tuff powder is 15% under steam curing condition. When the proportion of stone powder replaces cement is too high, the mechanical properties will decrease substantially. This is because the increase in the proportion of stone powder in the cement cementing system leads to a significant decrease in the content of cement slurry, a decrease in the degree of hydration, a

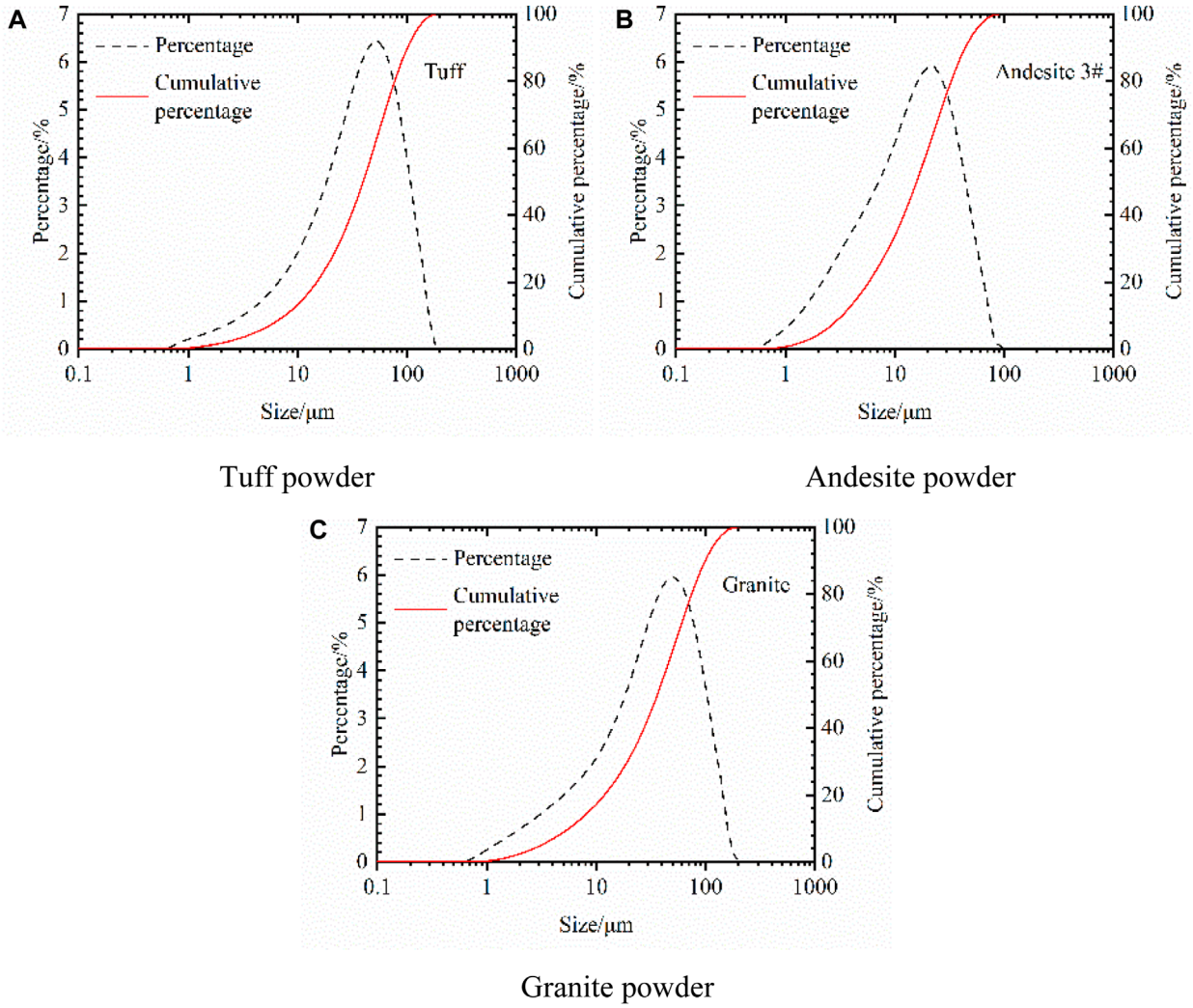

FIGURE 1
Size distribution curve of igneous rock powder. **(A)** Tuff powder; **(B)** Andesite powder; **(C)** Granite powder.

decrease in hydration products, and a decrease in strength on a macro level.

The application of igneous rock powder in cement concrete can not only reduce the amount of cement raw materials, reduce the environmental pollution caused by a large amount of CO_2 produced in the cement production process, but also can use local materials, save transportation costs, and avoid long-term accumulation of waste stone powder to the environment damage, improve resource utilization efficiency, and promote the development of circular economy. In view of this, the effects of tuff powder, granite powder and andesite powder on the fluidity, flexographic strength and compressive strength of cement slurry on the working and mechanical properties of the cement composite gelling system were investigated. In addition, the hydration characteristics and microscopic morphology were characterized by TG-DSC, Nanoindentation, X-ray diffraction (XRD) and scanning electron microscopy (SEM). By analyzing and evaluating the effect of the amount of igneous rock powder on the properties of cement composite cementing system, it provides reference value for the development and utilization of igneous rock.

2 Materials and method

2.1 Raw materials

The cement is made of P.O 42.5 grade Portland cement of Conch brand from Shaanxi Province. Andesite powder, tuff powder and granite powder are all made from igneous rocks in southwest China after grinding. The chemical composition of raw materials is shown in Table 1. The sand used is ISO standard sand produced by Xiamen Aisiou Standard Sand Co. Use laboratory tap water. (Note: IRP stands for Igneous Rock Powder; AP stands for Andesite Powder; TP stands for Tuff Powder; GP stands for Granite Powder).

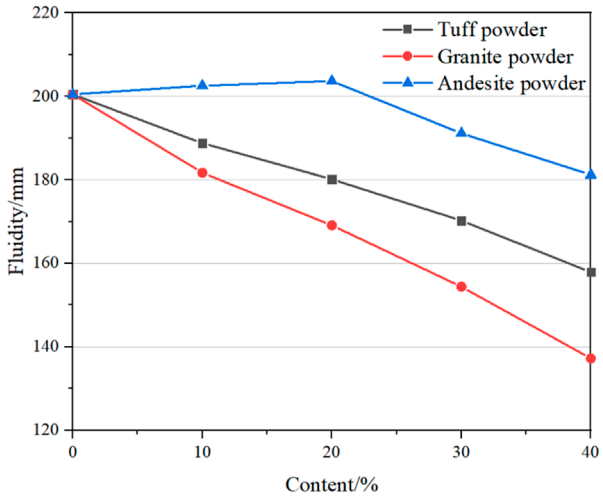

FIGURE 2
Fluidity of mortar of IRP-OPC compound cementing system.

Figure 1 shows the particle size distribution curves of tuff powder, granite powder and andesite powder respectively. The three types of igneous rocks were first prefabricated into crushed pieces with a grain size of less than 1 cm and then milled. The specific surface areas of granite powder, tuff powder and andesite powder after 1 h milling are 425.80 cm^2/g, 474.60 cm^2/g, and 756.12 cm^2/g. It can be seen from the particle size distribution curves of the three igneous rock powders that the particle size distribution of granite, tuff, andesite and fly ash has only one concentrated peak, indicating that the particle size distribution of the four powders is relatively concentrated. The difference is that the particle size of granite powder and tuff powder is mainly concentrated in about 50 μm, while the particle size of Andesite rock powder is mainly concentrated in about 20 μm, indicating that the particle size of Andesite powder is smaller than that of granite and tuff.

2.2 Mix ratio design

In order to clearly compare the effect of igneous powder content on cement paste properties, three igneous powders were selected for this study. Since the pre-tests have approximately defined the optimum dosing at around 10%, igneous rock was set to replace 0% (control), 5%, 10%, 15%, 20%, 30%, and 40% (mass fraction) of the cement in a single mixing condition. The water-cement ratio in the test was 0.50. The raw material ratios are specified in Table 2.

2.3 Fluidity test

Fluidity is an important index to evaluate the workability of cement slurry. The fluidity test of cement mortar in the composite cementitious system of igneous rock powder and cement was conducted in accordance with GB/T 2419: The method for fluidity of cement mortar (GB/T 2419-2005, 2005). The fluidity of cement mortar is measured by cement mortar fluidity tester. After jumping 25 times at the frequency of 1 time per second, the maximum diameters of the two perpendicular directions of the bottom surface of the cement mortar are measured, and the average value is the fluidity of the cement composite cementing system.

2.4 Mechanical property test

The mechanical properties of concrete are important parameters to evaluate the feasibility and rationality of structural design. In order to study the influence of igneous rock powder on the mechanical properties of cement composite cementitious system, The mechanical properties test was conducted in accordance with GB/T 17671: The method cement mortar strength (ISO method) (GB/T 17671-2021, 2021). P.O 42.5 Portland cement was used to prepare cement mortar with water-cement ratio (w/c) of 0.5 according to the designed mix ratio. The cement mortar was put into 40 mm × 40 mm × 160 mm cast iron mold and cured in the room at 95% relative humidity and (20 ± 2)°C for 24 h. The samples were demoulded and placed in a water curing box to be cured at 7 and 28 days of age for mechanical properties testing. There were 3 parallel specimens in each group. The arithmetic average of the test values of 3 parallel specimens was used as the strength value of each group of specimens.

2.5 Microscopic test

For microscopic testing, 15 mm × 15 mm × 15 mm net mortar specimens were made in the same proportions, maintained under the same conditions as the mortar and cured for 7 days. After curing, the centre portion of the fragments was immersed in ethanol for 24 h and then dried at 60°C for 24 h and subsequently ground to a fine powder. TG-DSC analysis was carried out using a thermogravimetric analyser model Q500IR from TA Instruments. The temperature range was from 25°C to 800°C with a heating rate of 10°C/min. The specific surface area was measured using a specific surface area analyser model ASAP 2420 from Micromeritics. The phase analysis of the prepared powder samples was carried out using an X-ray diffractometer model D8 Advance from AXS. The samples were scanned stepwise at 0.5° intervals at a scanning rate of 13°/minute and at scanning angles from 15° to 90°. A Hitachi model SU8010 scanning electron microscope was used to study the effect of IRP doping on the microstructural characteristics of IRP-OPC. Samples with edge lengths not exceeding 10 mm were intercepted from the mortar specimens. The samples were then soaked in anhydrous ethanol for 3 days to stop hydration and vacuum dried at 60°C for 24 h.

3 Results and discussion

3.1 Fluidity

Figure 2 shows the variation of the flowability of IRP-OPC composite materials with different amounts of various igneous rocks. It is observed that with an increase in the content of TP and GP, the flowability of cement mortar linearly

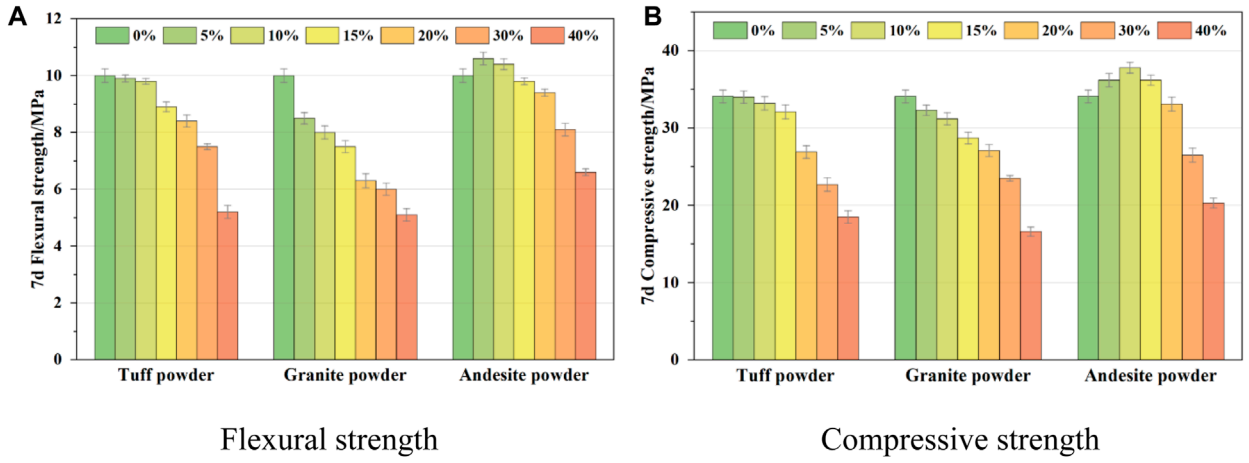

FIGURE 3
Mechanical properties of IRP-OPC composite system at the hydration age of 7 days. **(A)** Flexural strength; **(B)** Compressive strength.

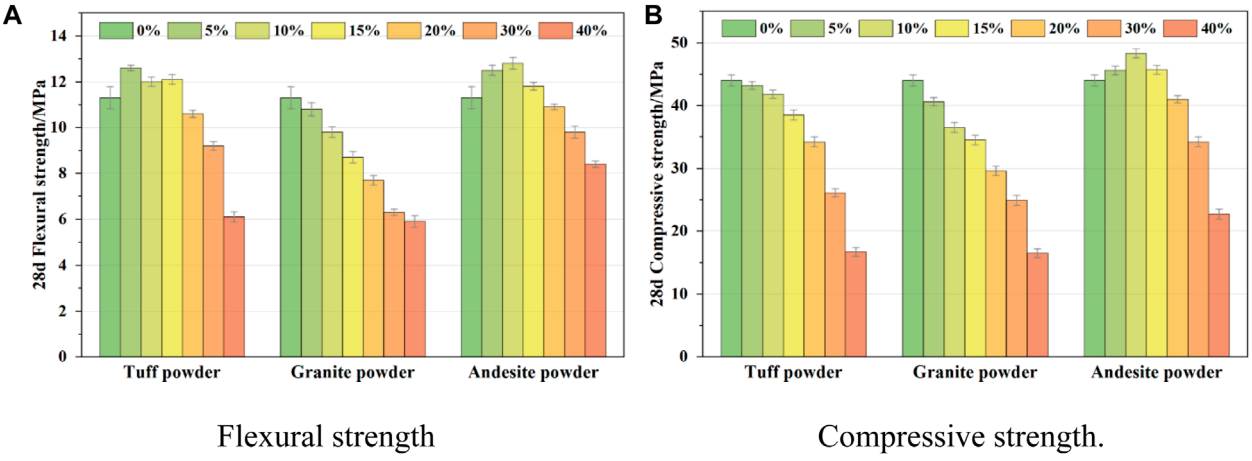

FIGURE 4
Mechanical properties of IRP-OPC composite system at the hydration age of 28 days. **(A)** Flexural strength; **(B)** Compressive strength.

decreases. However, the flowability with the addition of AP exhibits a different pattern. Before a 20% content, the flowability of mortar increases with the increase in content, but after reaching a 20% content, the flowability gradually decreases. TP has a laminar structure, and GP also contains a layered mineral structure composed of mica. The crystal structure of these materials determines their strong interlayer adsorption capacity, leading to the formation of agglomerates near particles due to the adsorption of a large amount of free water and admixtures, thus reducing the dispersibility of cement paste. Additionally, this agglomeration increases the sliding resistance between cement particles, significantly reducing the flowability of mortar (Huang et al., 2020). A small amount of AP can improve the flowability of mortar because the andesite powder has a small particle size, which can effectively disperse in cement particles, acting as a dispersant to prevent the formation of "coagulation structure" during cement hydration reactions. However, with the continuous increase in AP content, the overall specific surface area of the powder particles significantly increases, leading to agglomeration between powder particles. Therefore, the flowability of cement mortar rapidly decreases (Xiao et al., 2023).

3.2 Mechanical properties

The mechanical properties of IRP-OPC composite system were depicted in Figures 3, 4, representing the respective hydration ages of 7 days and 28 days.

At the hydration age of 7 days, the inclusion of TP and GP in the cement composite system leads to a decrease in both the flexural strength and compressive strength. Conversely, the appropriate addition of AP results in an increase in the early flexural strength and compressive strength of the cement mortar. The compressive and flexural strengths of the specimens are significantly increased when the dosage of AP is 15% or less, and the strength decreases rapidly

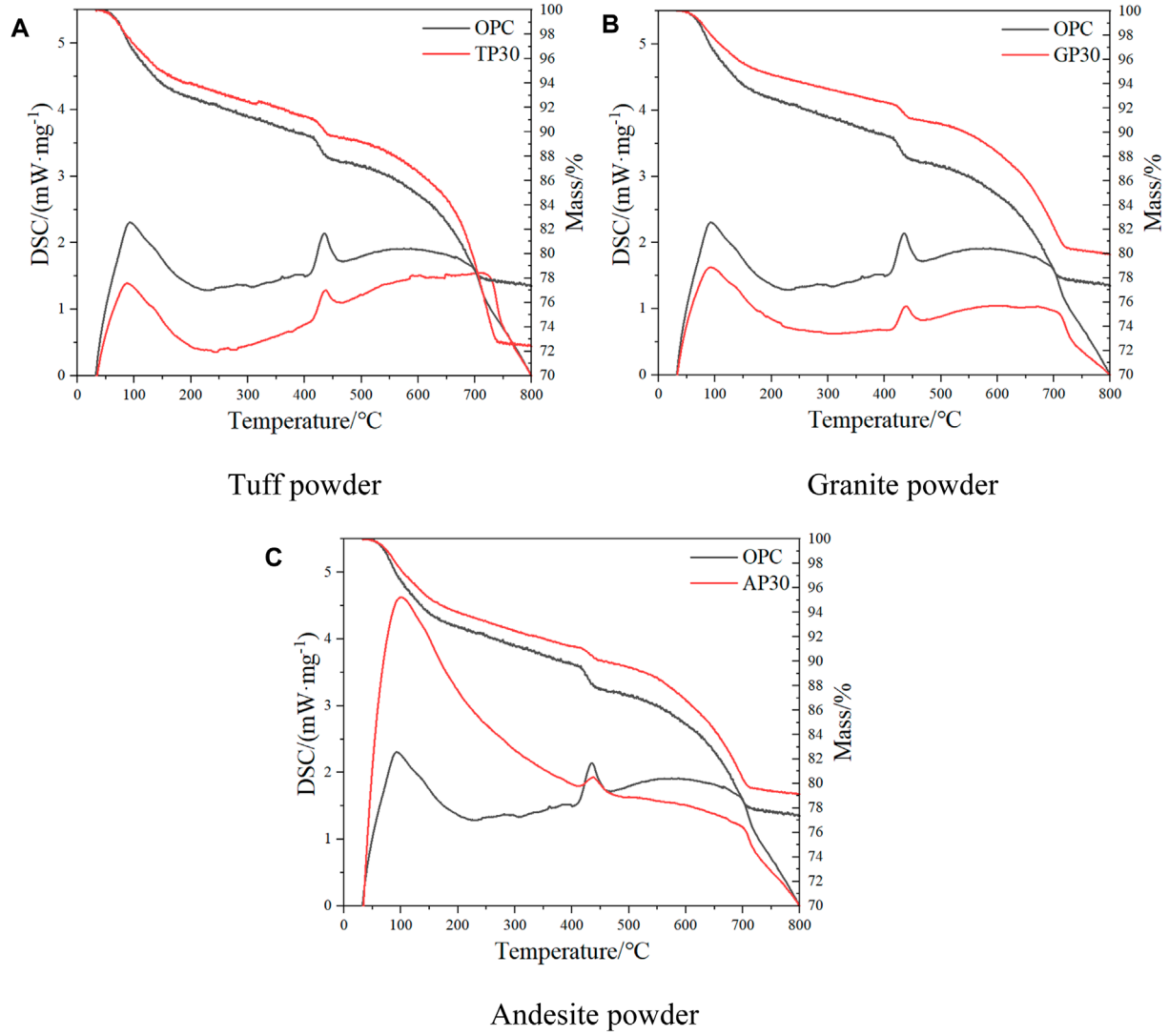

FIGURE 5
The TG/DSC curve of the hardened paste of IRP-OPC composite system at the hydration age of 7 days. **(A)** Tuff powder; **(B)** Granite powder; **(C)** Andesite powder.

when the dosage is 15% or more. The initial reactivity of the IRP is relatively low, and the involvement of IRP with limited pozzolanic activity in the early hydration reaction is restricted. Both tuff and granite, being inert mineral admixtures with low early activity and larger particle sizes, exhibit a lower degree of early hydration participation. Additionally, their filling effect is not prominent, the development of early strength is impeded (Peng et al., 2017). However, TP possessed a laminar structure, which formed an intercalated structure within the cement composite system and provided a certain level of flexural strength support. The particle size of AP is smaller than that of TP and GP, and the filling effect is fully exerted by the low content of AP, and AP particles can be filled into the structural gaps with hydration products to improve the compactness of the system.

At a hydration age of 28 days, the compressive strength of the cement composite system still decreases due to the addition of TP and GP. However, when AP was doped it was found that the compressive and flexural strengths of the specimens increased significantly at dosages up to 15%. In particular, at a dosage of 10%, the compressive strength is 48.3 MPa, which is 9.8% higher compared to the reference cement, and the flexural strength is 12.8 MPa, which is 13.3% higher compared to the reference cement. When the dosage exceeds 15%, the strength of the specimen decreases significantly with the increase of dosage. It is worth noting that when the TP dosage is below 15%, although the compressive strength of the specimen will be reduced, when the flexural strength is obviously improved, up to 12.6 MPa, compared with the benchmark cement by 11.5%. The addition of IRP results in a reduction in the content of cement slurry, hydration products, and system density. The lamellar structure of tuff powder particles enables strong adsorption on cement particles. At the microscopic level, tuff powder particles can form an intercalation structure with cement particles, the bending strength is significantly improved (Zeyad et al., 2020; Özkan et al., 2022). While AP exhibits high

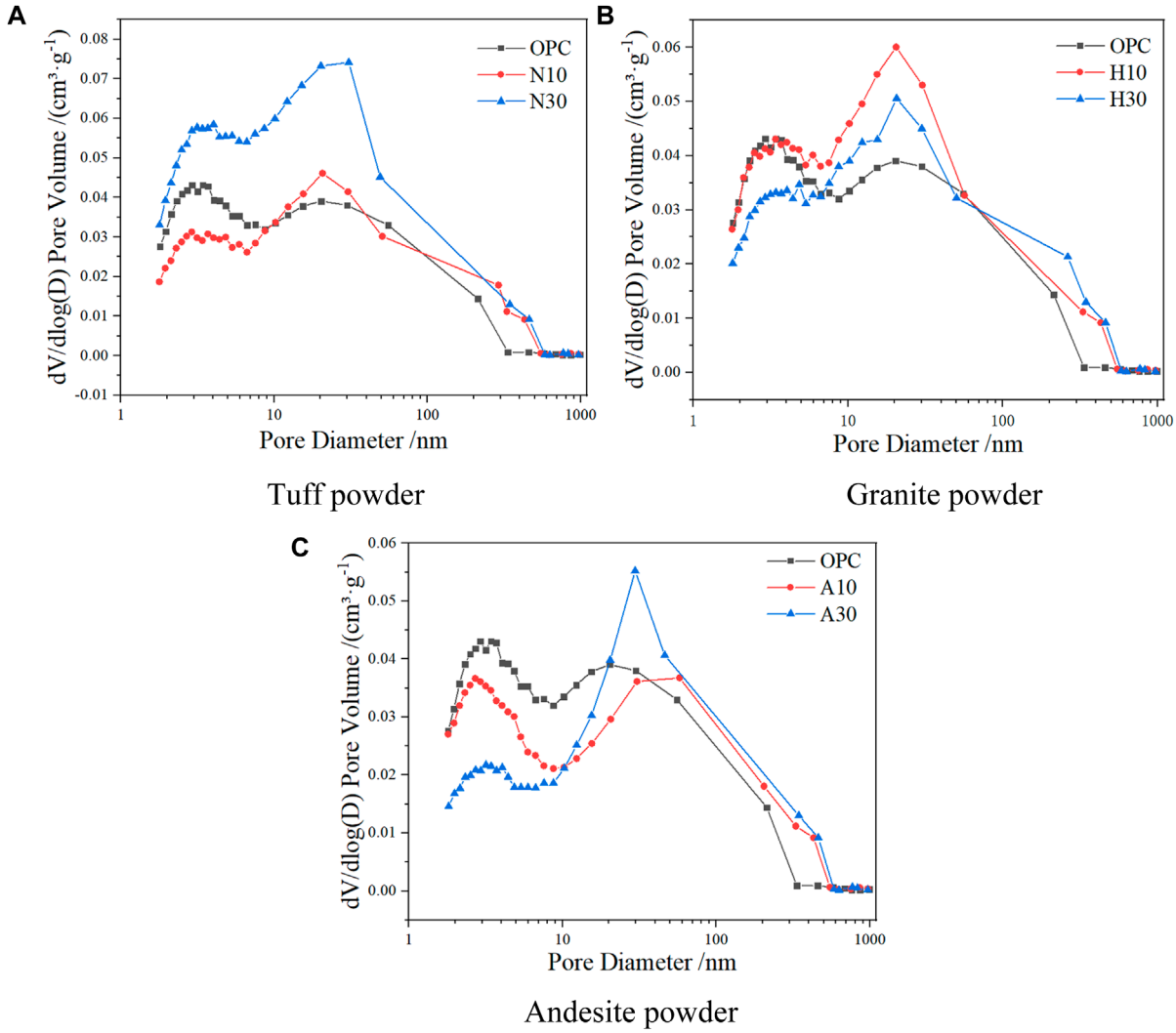

FIGURE 6
The pore distribution curves of hardened paste of igneous rock powder-cement composite system at hydration age of 7 days. **(A)** Tuff powder; **(B)** Granite powder; **(C)** Andesite powder.

activity and can participate in hydration reactions during later stages. The filling effect of the stone powder and the formation of the C-S-H gel phase improved the internal compactness of the specimen to some extent, resulting in an increase in the mechanical properties (Çelikten, 2021). When the dosage exceeds 15%, AP and TP replace a large amount of cement, and the strength growth mechanism of AP and TP does not offset the negative effect of the decrease in the proportion of cement, so the strength decreases significantly.

3.3 TG/DSC analysis

TG/DSC were employed to further investigate the hydration process of the cement composite system incorporating igneous stone powder. As depicted in Figures 5A–C, the addition of igneous rock does not significantly alter the thermal decomposition stages of the cement composite system, but it does affect the thermal gravimetric range of each stage. TG curves exhibit three weight loss steps, indicating three occurrences of thermogravimetry and corresponding to three endothermic peaks in DSC curves. Notably, there is a distinct endothermic peak observed between 75°C and 120°C, corresponding to the dehydration of AFt crystals at approximately 100°C and AFm crystals at around 120°C. In the early stages of the hydration reaction, weight loss primarily results from the evaporation of calcium silicate hydrate (C-S-H), Ettringite (AFt), and free water. In the temperature range of 400–500°C, the thermo-gravimetric stage is mainly attributed to the thermal decomposition of calcium hydroxide [$Ca(OH)_2$], accompanied by a noticeable endothermic peak in the corresponding DSC curve. The heat absorption peak observed between 680°C and 750°C is attributed to the thermal decomposition of $CaCO_3$. The dehydration process of the C-S-H gel occurs throughout the entire heating process, hence no distinct weight loss step or heat absorption peak

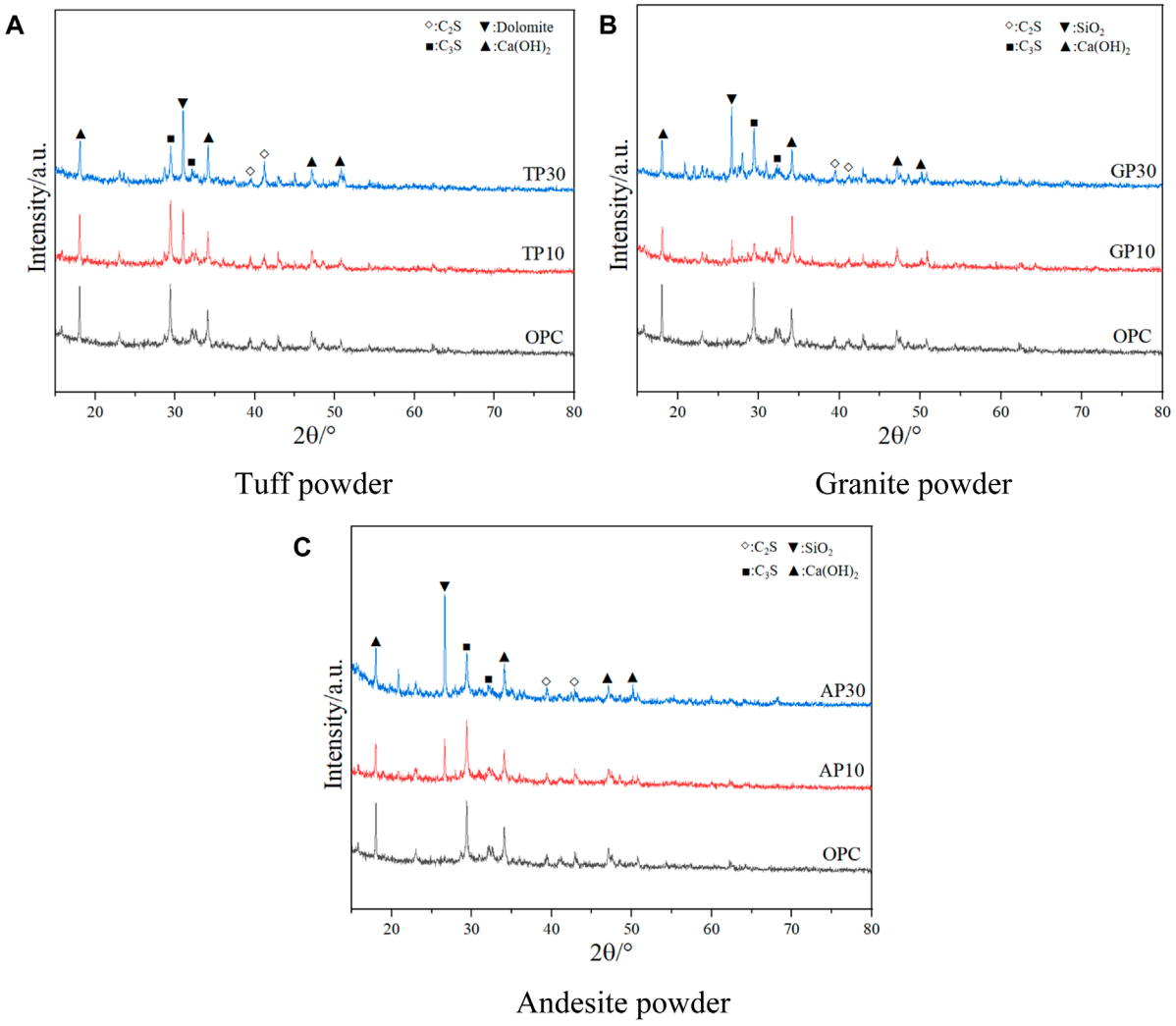

FIGURE 7
The XRD pattern of hardened paste of igneous rock powder-cement composite system at hydration age of 28 days. **(A)** Tuff powder; **(B)** Granite powder; **(C)** Andesite powder.

is observed in the figure. The involvement of mineral admixtures in the cement hydration reaction leads to the consumption of $Ca(OH)_2$ and promotes the formation of hydration products. The extent of mineral admixture participation in the cement hydration reaction can be estimated by evaluating the area of the $Ca(OH)_2$ endothermic peak (Kong et al., 2023; Llorens et al., 2023). The extent of participation of mineral admixtures in cement hydration reaction can be predicted by the area of the endothermic peak of $Ca(OH)_2$.

As illustrated in Figure 5C, In the range of 70–110°C, the endothermic peak area of AP samples is larger than that of TP and GP samples, indicating that AFt crystal and free water content are higher in AP system. In the range of 420°C–470°C, the area of C-H absorption peak is the smallest, and the range of thermogravimetric loss in TG curve is lower, indicating that the content of $Ca(OH)_2$ in the cement composite system was reduced by the addition of AP, as indicated by the smallest area of the C-H absorption peak and a lower range of thermogravimetric loss in the TG curve. This reduction occurred because AP consumed $Ca(OH)_2$, actively participated in the hydration reaction, and facilitated the formation of calcium-silicate-hydrate (C-S-H) gel. In contrast, GP and TP exhibited low activity and were classified as inert volcanic ash mineral admixtures. Due to the difficulty in releasing sufficient active SiO_2 and Al_2O_3, their powder particles had limited capacity to consume $Ca(OH)_2$, resulting in a lower degree of participation in the hydration reaction (Liu M. et al., 2021). Therefore, under the same dosage, the late strength of AP-OPC composite system is higher.

3.4 N_2 adsorption-desorption curve (BET)

Figure 6 illustrates the distribution of apertures in the IRP-OPC composite system. It is well-known that large pores and capillary

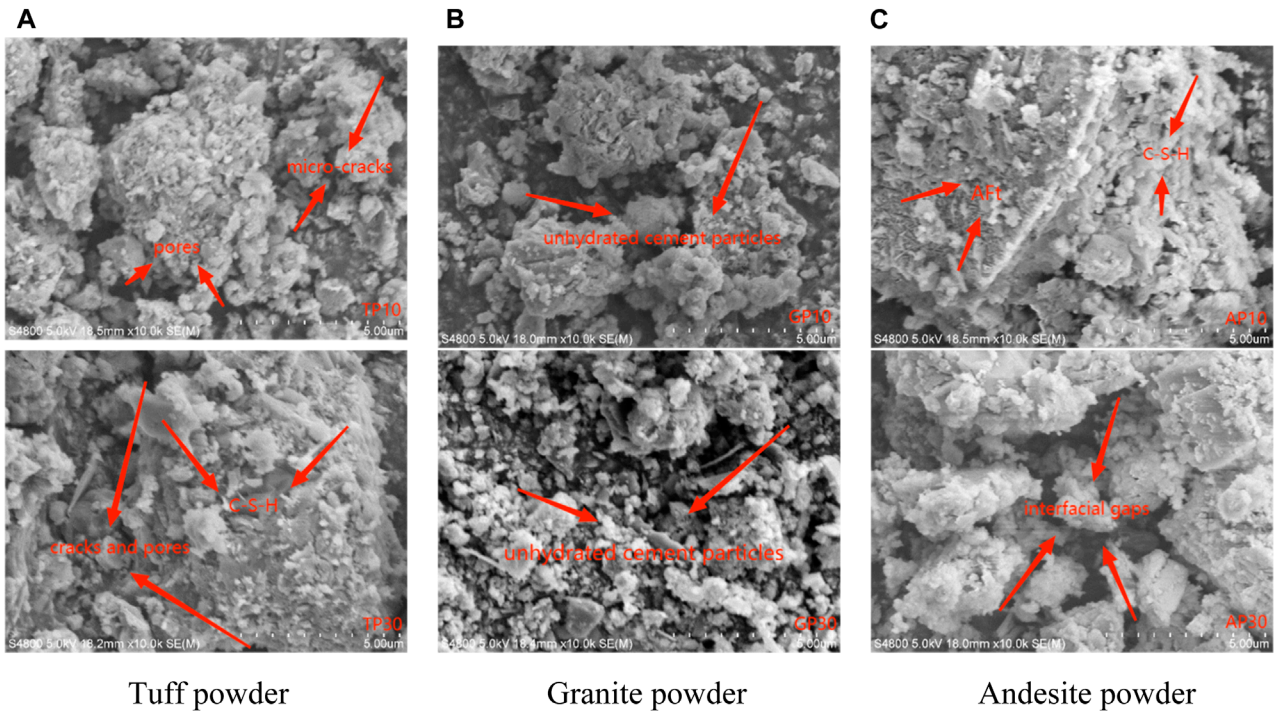

FIGURE 8
The SEM image of the hardened mortar of igneous rock powder and cement composite system at hydration age of 7 days. **(A)** Tuff powder; **(B)** Granite powder; **(C)** Andesite powder.

pores (>100 nm) have detrimental effects on the mechanical strength and water tightness of cement slurry (Hu and Li, 2015; Zhang et al., 2022; Liao et al., 2023). Therefore, a higher proportion of smaller pores and capillary pores (<10 nm) leads to a denser structure of cement paste (Sun et al., 2022). The average pore diameter of TP10 and GP10 was measured to be 11.1216 cm^3/g and 10.5846 cm^3/g. In contrast, the average pore diameter of AP10 samples was smaller than that of the control group, measuring 9.3944 cm^3/g. As shown in the figure, the addition of TP and GP significantly increased the proportion of large pores (10 nm–100 nm) in the cement system, resulting in a higher porosity of the system. On the other hand, the inclusion of 10% AP content shifted the pore size distribution towards smaller pores (<10 nm) and significantly reduced the content of large pores. TP and GP possess larger pore sizes and are considered inert pozzolanic active admixtures. Their involvement in hydration reactions during the early stage is limited, and their ability to fill the internal pores of the cement slurry is inadequate. Nevertheless, owing to its smaller pore size, AP actively engaged in hydration reactions, resulting in the production of more C-S-H. In conjunction with other hydration products, AP effectively filled the structural voids and pores within the cement slurry, refining its pore structure and enhancing the system's density. Consequently, the AP-OPC composite exhibited higher compressive strength in comparison to the TP-OPC and GP-OPC composites (Belebchouche et al., 2021). On a macroscopic level, the late-stage compressive strength surpassed that of the TP-OPC and GP-OPC composite systems.

3.5 XRD analysis

Figure 7 presents the XRD pattern of the binary composite gelling system composed of igneous stone powder and cement. The XRD pattern primarily exhibited diffraction characteristic peaks of hydration products, such as calcium hydroxide [$Ca(OH)_2$], calcium vanadate (AFt), and tricalcium silicate (C_3S). The igneous rock powder displayed low early activity and had limited participation in the hydration reaction, resulting in a small yield of AFt and AFm and low diffraction peak intensity. At $2\theta = 18°$, the peak intensity of the C-H diffraction was reduced with the incorporation of IRP; At $2\theta = 26.6°$, the diffraction peak intensity of SiO_2 gradually increased with an increase in AP and GP incorporation. The incorporation of IRP resulted in a decrease in the cement slurry content in the cement system, thereby impeding the formation of hydration products such as $Ca(OH)_2$. At low concentrations, the addition of AP resulted in a reduction in the diffraction peaks of both C-H and SiO_2, indicating that the low content of AP did not significantly diminish the cement slurry content in the cement composite gelling system. At the same time, sufficient SiO_2 and other active ingredients are provided to participate in the hydration reaction. The active SiO_2 and Al_2O_3 present in the stone powder particles fully reacted with $Ca(OH)_2$ in the cement system and actively participated in the hydration reaction of C_3S and C_2S, leading to the formation of a substantial amount of C-S-H gel (Zhou et al., 2023; Geng et al., 2024). Consequently, AP did not substantially impede the degree of cement hydration reaction at low concentrations, and the strength is even improved (Cao et al., 2016; Kawabata et al., 2019).

3.6 SEM analysis

Figure 8 presents the SEM image of the igneous rock powder-cement composite gelling system, allowing for the evaluation of the influence of different igneous rock powders on the cement slurry hydration process through the analysis of the micro-structure of the cement composite system. Figure 8A corresponds to SEM plots of hardened mortar with 10% and 30% TP alone, Figure 8B corresponds to SEM plots of hardened mortar with 10% and 30% TP alone, and Figure 8C corresponds to SEM plots of hardened mortar with 10% and 30% TP alone. As depicted in Figure 8A, there are unhydrated cement particles present in the interface region of the TP10 sample, alongside micro-cracks and pores. The TP30 sample exhibits a small amount of amorphous C-S-H gel in the interface region, along with noticeable cracks and large pores, indicating a relatively loose system structure. This phenomenon can be attributed to the inert nature of tuff powder and granite powder, which are mineral admixtures with low early reactivity. The system contains a limited amount of active SiO_2, which hampers its complete reaction with the $Ca(OH)_2$ present. Consequently, the cement stone structure becomes porous, leading to the formation of numerous microcracks in the slurry and a subsequent reduction in early strength (Ben Haha et al., 2007). The AP10 sample exhibited a distinct presence of flocculent C-S-H gel and some needle-rod ettringite (AFt) on its surface. As the mixing amount increased, the interfacial gaps in the AP30 cement slurry structure significantly expanded, leading to the dispersion of unhydrated cement particles between the gaps and the surface of the structure. This dispersion prevented the effective formation of a dense filling structure. These observations indicate that at low concentrations, IRP does indeed exhibit a nucleation effect during the early hydration stage, thereby promoting cement hydration. This effect can be attributed to the adsorption capacity of the IRP surface, which absorbs free calcium ions from the solution. When the solution becomes supersaturated, CH crystals and C-S-H gel begin to form on the surface of the stone powder, resulting in a decrease in the concentration of Ca^{2+} around C_3S. This decrease, in turn, promotes cement hydration. However, as the content of stone powder increases, the cement slurry content in the system gradually decreases, leading to a reduction in the generation of hydration products. Consequently, the C-S-H gel fails to effectively crosslink into a network structure, resulting in a decrease in the density of the system (Mei and Liu, 2003; Fang et al., 2023; Hu et al., 2023). Therefore, it is best to control the content of igneous rock powder in the range of 5%–15%.

4 Conclusion

This paper explores the feasibility of replacing part of cement as cementitious material by igneous rock powder through the macro and micro properties of mortar. It is finally found that andesite is one of the effective replacement materials for cement. When the strength requirement is low, andesite and granite can also be used to replace a small portion of cement as cementitious material. Replacing cement with igneous rock powder can not only guarantee that the strength of mortar meets the requirements, but also reduce the project cost and improve the utilisation rate of igneous rock powder. The main conclusions are as follows.

(1) The flowability of cement mortar initially increased and then decreased with the addition of AP. Conversely, the inclusion of TP and GP gradually decreased the flowability of the cement mortar.
(2) The early and late compressive and flexural strengths of the specimens were significantly improved when the dosage of AP was up to 15% or less, and the 28-day compressive strength could reach 48.3 MPa and the 28-day flexural strength could reach 12.8 MPa. The strength decrease was also smaller when the dosage of TP and GP was up to 15%, and even TP could improve the late flexural strength of the specimens.
(3) Compared to other types of inert rock powder (IRP), the addition of AP during cement hydration demonstrated superior effects on particle filling and activity in the later stages. AP actively participated in the reaction, effectively filling structural voids with powder particles and hydration products like C-S-H gel. This led to the refinement of the cement slurry's pore structure and improved density.

Data availability statement

The original contributions presented in the study are included in the article/Supplementary material, further inquiries can be directed to the corresponding authors.

Author contributions

ZL: Formal Analysis, Writing–original draft. ZZ: Writing–original draft, Data curation. FM: Data curation, Writing–review and editing. WD: Methodology, Writing–review and editing. XC: Data curation, Methodology, Writing–original draft. ZH: Writing–review and editing, Software. BG: Writing–review and editing, Funding acquisition, Methodology.

Funding

The author(s) declare that financial support was received for the research, authorship, and/or publication of this article. This research was funded by Key R&D and transformation plan of Qinghai Province (2021-SF-140).

Conflict of interest

Authors ZL, ZZ, and FM were employed by China First Highway Engineering Co., Ltd.

The remaining authors declare that the research was conducted in the absence of any commercial or financial relationships that could be construed as a potential conflict of interest.

Publisher's note

References

Ahmad, M. R., and Chen, B. (2018). Effect of silica fume and basalt fiber on the mechanical properties and microstructure of magnesium phosphate cement (MPC) mortar. *Constr. Build. Mater.* 190, 466–478. doi:10.1016/j.conbuildmat.2018.09.143

Antolik, A., Dąbrowski, M., and Jóźwiak-Niedźwiedzka, D. (2023). Petrographic evaluation of aggregate from igneous rocks: alkali–silica reaction potential. *Minerals* 13, 1004. doi:10.3390/min13081004

Belebchouche, C., Moussaceb, K., Bensebti, S. E., Aït-Mokhtar, A., Hammoudi, A., and Czarnecki, S. (2021). Mechanical and microstructural properties of ordinary concrete with high additions of crushed glass. *Materials* 14, 1872. doi:10.3390/ma14081872

Ben Haha, M., Gallucci, E., Guidoum, A., and Scrivener, K. (2007). Relation of expansion due to alkali silica reaction to the degree of reaction measured by SEM image analysis. *Cem. Concr. Res.* 37 (8), 1206–1214. doi:10.1016/j.cemconres.2007.04.016

Bentz, D. P., Ferraris, C. F., Jones, S. Z., Lootens, D., and Zunino, F. (2017). Limestone and silica powder replacements for cement: early-age performance. *Cem. Concr. Compos.* 78, 43–56. doi:10.1016/j.cemconcomp.2017.01.001

Cao, X., Xia, D. C., and Yin, W. X. (2016). Influences of tuff powder and VF anti-cracking agent on hydration characteristics of cement paste. *Hongshui River* 35, 38–41. doi:10.3969/j.issn.1001-408X.2016.01.009>

Çelikten, S. (2021). Mechanical and microstructural properties of waste andesite dust-based geopolymer mortars. *Adv. Powder Technol.* 32 (1), 1–9. doi:10.1016/j.apt.2020.10.011

Dobiszewska, M., Bagcal, O., Beycioğlu, A., Goulias, D., Köksal, F., Płomiński, B., et al. (2023). Utilization of rock dust as cement replacement in cement composites: an alternative approach to sustainable mortar and concrete productions. *J. Build. Eng.* 69, 106180. doi:10.1016/j.jobe.2023.106180

Elmoaty, A. (2013). Mechanical properties and corrosion resistance of concrete modified with granite dust. *Constr. Build. Mater.* 47, 743–752. doi:10.1016/j.conbuildmat.2013.05.054

Fang, Y., Zhang, L., Li, L., Zhao, M., Wang, Q., and Mei, Y. (2023). Preparation of nano-sized C-S-H and its acceleration mechanism on Portland cement hydration at different temperatures. *Materials* 16, 3484. doi:10.3390/ma16093484

GB/T 17671-2021 (1999) *Test method ofcement mortar strength(ISO method)*. Beijing: Standards Press of China.

GB/T 2419-2005 (2005) *Test method for fluidity of cement mortar*. Beijing: Standards Press of China.

Geng, Z. C., Tang, S. W., Wang, Y., A., H., Wu, K., He, Z., et al. (2024). Stress relaxation properties of calcium silicate hydrate: a molecular dynamics study. *J. Zhejiang University-SCIENCE A* 25 (2), 97–115. doi:10.1631/jzus.a2300476

Hu, C., and Li, Z. (2015). A review on the mechanical properties of cement-based materials measured by nanoindentation. *Constr. Build. Mater.* 90, 80–90. doi:10.1016/j.conbuildmat.2015.05.008

Hu, Y., Li, K., Zhang, B., and Han, B. (2023). Development of cemented paste backfill with superfine tailings: fluidity, mechanical properties, and microstructure characteristics. *Materials* 16, 1951. doi:10.3390/ma16051951

Huang, L., Yan, P., and Liu, Y. (2020). Effect of alkali content in cement on the fluidity and structural build-up of plasticized cement pastes. *Constr. Build. Mater.* 253, 119180. doi:10.1016/j.conbuildmat.2020.119180

Kawabata, Y., Dunant, C., Yamada, K., and Scrivener, K. (2019). Impact of temperature on expansive behavior of concrete with a highly reactive andesite due to the alkali–silica reaction. *Cem. Concr. Res.* 125, 105888. doi:10.1016/j.cemconres.2019.105888

Kong, C., Zhou, B., Guo, R., Yan, F., Wang, R., and Tang, C. (2023). Preparation and micromechanics of red sandstone–phosphogypsum–cement composite cementitious materials. *Materials* 16, 4549. doi:10.3390/ma16134549

Liao, Y. S., Wang, S. C., Wang, K. J., Qunaynah, S. A., Yuan, Z., Xu, P., et al. (2023). A study on the hydration of calcium aluminate cement pastes containing silica fume using non-contact electrical resistivity measurement. *J. Mater. Res. Technol.* 24, 8135–8149. doi:10.1016/j.jmrt.2023.05.080

Liu, M., Hong, S., Wang, Y., Zhang, J., Hou, D., and Dong, B. (2021b). Compositions and microstructures of hardened cement paste with carbonation curing and further water curing. *Constr. Build. Mater.* 267, 121724. doi:10.1016/j.conbuildmat.2020.121724

Liu, S., Liang, X., Wang, H., Liu, M., and Ouyang, L. (2022). Effects of tuff powder on the hydration properties of cement-based materials under high temperature. *Sustainability* 14, 14691. doi:10.3390/su142214691

Liu, S. H., Fang, P. P., Wang, H. L., Kong, Y., and Ouyang, L. (2021a). Effect of tuff powder on the hydration properties of composite cementitious materials. *Powder Technol.* 380, 59–66. doi:10.1016/j.powtec.2020.11.029

Llorens, J., Julián, F., Gifra, E., Espinach, F. X., Soler, J., and Chamorro, M. À. (2023). An approach to understanding the hydration of cement-based composites reinforced with untreated natural fibers. *Sustainability* 15, 9388. doi:10.3390/su15129388

Mei, G. X., and Liu, W. B. (2003). SEM analysis of the hydrate of tuff grout and phosphorus-slag grout. *Concrete* 2003, 49–51. doi:10.3969/j.issn.1002-3550.2003.03.015

Menéndez, G., Bonavetti, V., and Irassar, E. F. (2003). Strength development of ternary blended cement with limestone filler and blast-furnace slag. *Cem. Concr. Compos.* 25, 61–67. doi:10.1016/s0958-9465(01)00056-7

Özkan, Ş., and Ceylan, H. (2022). The effects on mechanical properties of sustainable use of waste andesite dust as a partial substitution of cement in cementitious composites. *J. Build. Eng.* 58, 104959. doi:10.1016/j.jobe.2022.104959

Peng, S. T., Li, X., Wu, Z. Y., Chen, J., and Lu, X. (2017). Study of the key technologies of application of tuff powder con-crete at the Daigo hydropower station in Tibet. *Constr. Build. Mater.* 156, 1–8. doi:10.1016/j.conbuildmat.2017.08.138

Piasta, W., Góra, J., and Turkiewicz, T. (2016). Properties and durability of coarse igneous rock aggregates and concretes. *Constr. Build. Mater.* 126, 119–129. doi:10.1016/j.conbuildmat.2016.09.022

Qaidi, S., Najm, H. M., Abed, S. M., Ahmed, H. U., Al Dughaishi, H., Al Lawati, J., et al. (2022). Fly ash-based geopolymer composites: a review of the compressive strength and microstructure analysis. *Materials* 15, 7098. doi:10.3390/ma15207098

Sun, H., Lian, W., Zhang, X., Liu, W., Xing, F., and Ren, J. (2022). Synthesis and processing parameter optimization of nano-belite via one-step combustion method. *Materials* 15, 4913. doi:10.3390/ma15144913

Wang, J., Xue, C., Zhang, Y., Li, Q., Han, Y., and Qiao, H. (2023). Study of early-age hydration, mechanical properties development, and microstructure evolution of manufactured sand concrete mixed with granite stone powder. *Materials* 16, 4857. doi:10.3390/ma16134857

Xiao, T., Yu, Z., Liu, F., Dai, X., and Sun, J. (2023). Study on slurry flow characteristics and diffusion law of superfine cement-based composite grouting material. *Processes* 11, 1906. doi:10.3390/pr11071906

Ying, L., Yu, H., Zheng, L., Wen, J., Wu, C., and Tan, Y. (2013). Compressive strength of fly ash magnesium oxychloride cement containing granite wastes. *Constr. Build. Mater.* 38 (1-7), 0950–0618. doi:10.1016/j.conbuildmat.2012.06.016

Zeyad, A. M., Khan, A. H., and Tayeh, B. A. (2020). Durability and strength characteristics of high-strength concrete incorporated with volcanic pumice powder and polypropylene fibers. *J. Mater. Res. Technol.* 9 (1), 806–818. doi:10.1016/j.jmrt.2019.11.021

Zhang, Y., Liang, M., Gan, Y., and Çopuroğlu, O. (2022). Micro-mechanical properties of slag rim formed in cement–slag system evaluated by nanoindentation combined with SEM. *Materials* 15, 6347. doi:10.3390/ma15186347

Zhou, Y. F., Li, W. W., Peng, Y. X., Tang, S., Wang, L., Shi, Y., et al. (2023). Hydration and fractal analysis on low-heat Portland cement pastes using thermodynamics-based methods. *Fractal Fract.* 7, 606–633. doi:10.3390/fractalfract7080606